A novel technique of friction and material property measurement by tip test in cold forging

Y T Im*, S H Kang, and **J S Cheon**
Department of Mechanical Engineering, Korea Advanced Institute of Science and Technology, Daejeon, Republic of Korea

The manuscript was received on 29 November 2004 and was accepted after revision for publication on 20 June 2005.

DOI: 10.1243/095440505X32670

Abstract: Tip test experiments and simulations showed that the relationships between the tip distance, forming load, and shear friction factor were linear for all tested materials of aluminium alloys, steel, and copper. The ratio of the shear friction factor of the workpiece–die interface to that of the workpiece–punch interface was determined to be in the range of 23–60 per cent depending on the material. Also a logarithmic relation between the ratio of these two shear friction factors and the strain-hardening exponent of the material was found in the present investigation. Finally, it was clearly demonstrated that the tip test can be used to determine effectively the material property with decoupling of the friction effect in compression tests.

Keywords: tip test, friction, material characterization

1 INTRODUCTION

The finite element (FE) method has become an important analysis tool for bulk metal forming processes because of the advantages in time and cost savings. It is well known that reliability of such FE simulations depends on accurate material characterization and description of friction conditions which directly affect material flow, forming load requirement, die life, etc.

To date, simplified friction models commonly used for finite element (FE) simulations of metal forming processes are as follows [**1**].

1. The Coulomb friction model given by

$$\tau = -\mu p \tag{1}$$

2. The constant-shear-friction model given by

$$\tau = -m_{\mathrm{f}} k_{\mathrm{s}} \tag{2}$$

In these equations, τ, μ, p, m_{f}, and k_{s} are the frictional shear stress, friction coefficient, normal pressure, shear friction factor, and shear yield strength respectively of the material.

In general, the Coulomb friction model adequately represents the friction condition in sheet metal forming processes with low pressures while the constant-shear-friction model is commonly used for a description of the friction condition in bulk metal forming processes with relative high pressures. Therefore, the constant-shear-friction model was employed in the current investigation since the objective of this study is to determine the friction condition and material property for the cold-forming processes.

So far, many friction-testing methods have been proposed through the years. Among these, the ring compression test [**2**] has been widely used owing to its simplicity. However, it relies on non-linear calibration curves to characterize the friction condition, and shear friction factors obtained by this method may not always be suitable for simulating actual metal forming processes. This is because the shear friction factor varies during the deforming process depending on the measuring techniques and process conditions, as found in previous studies.

Thus, extrusion processes such as backward extrusion [**3**] and combined forward–backward extrusion [**4**] have been introduced to determine the friction condition for practical cold-forging

**Corresponding author: Department of Mechanical Engineering ME3227, Korea Advanced Institute of Science and Technology, CAMP Laboratory, 373-1 Guseong-dong, Yuseong-gu, Daejeon 305-701, Republic of Korea. email: ytim@webmail.kaist.ac.kr*

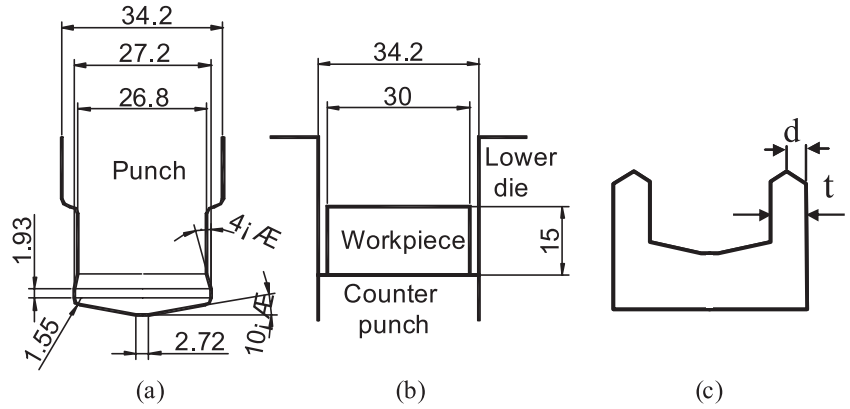

Fig. 1 Dimensions of (a) the axisymmetric punch and (b) the axisymmetric die used for the tip test (dimensions in millimetres) and (c) the deformed shape after tip test and definition of radial tip distance *d*

processes owing to the large surface expansion and high pressure distribution at the workpiece and die interfaces. However, these methods also require non-linear calibration curves and the test equipment is rather complex in design and operation.

Recently, Im *et al.* [**5**–**7**] proposed the 'tip test' in which a radial tip was formed on the extruded end of the workpiece simply to measure the friction level. In these earlier studies, it was found through experiments and FE simulations that both the radial tip distance and the maximum forming load increased linearly at higher levels of friction for a specimen of aluminium alloy Al6061-O. The effect of strain hardening on the frictional behaviour in the tip test was investigated further [**8**].

In the current study, tip test experiments and simulations with various aluminium alloys, carbon steel, and pure copper were conducted. According to the results, the linearity between the radial tip distance, forming load and shear friction factor was maintained for all materials investigated and the shear friction factor at the workpiece–lower die interface was in the range of 23–60 per cent of that at the workpiece–punch interface. In addition, a logarithmic relation between the ratio of the shear friction factor of the workpiece–die interface to that of the workpiece–punch interface and the strain-hardening exponent of the material was found. It is clearly demonstrated that the material property can be determined together with the shear friction factor by applying the tip test to the aforementioned materials with decoupling of the friction effect in compression tests.

2 TIP TEST EXPERIMENTS

Tip test experiments using aluminium alloys Al2024-O, Al5083-O, Al6061-O, and Al7075-O, annealed carbon steel AISI 1010, and pure copper C12100 were carried out to examine the linearity between the forming load and radial tip distance measured. The punch and dies used for the tip test experiments were made of tool steel alloy AISI D2 and polished to 0.08 μm in terms of R_a and coated with chromium. The dimensions of the punch and dies used in experiments are given in Fig. 1. The lubricants used in experiments were grease, drawing oil, soap, MoS_2, industrial oils with viscosity grades of VG22 and 100, and the household lubricant WD40. In the cases of tip tests with Al2024-O and AISI 1010, phosphate-coated specimens were used.

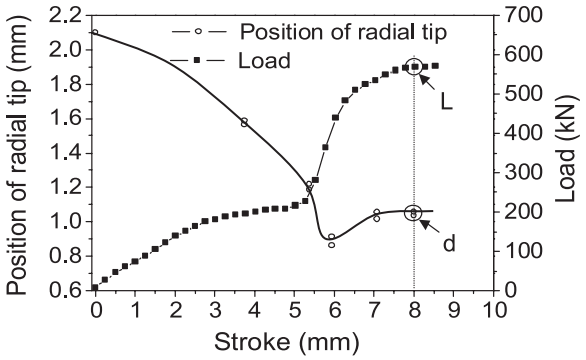

Fig. 2 Position of the radial tip from the inner wall of the lower die and the forming load according to the punch stroke

Figure 2 shows the position of the radial tip measured from the inner wall of the lower die and forming load according to the punch stroke obtained from the experiment with the Al2024-O specimen using the lubricant VG 100. The maximum forming load L and radial tip distance d were defined as the values when the punch stroke reached 8 mm.

Figure 3 shows the cross-sectional shapes of the finally deformed workpieces obtained from experiments on the Al2024-O specimen depending on the various lubricants used. The results clearly show that the radial tip distance varies depending on the friction conditions. In the present study, three experiments were carried out for each lubricant,

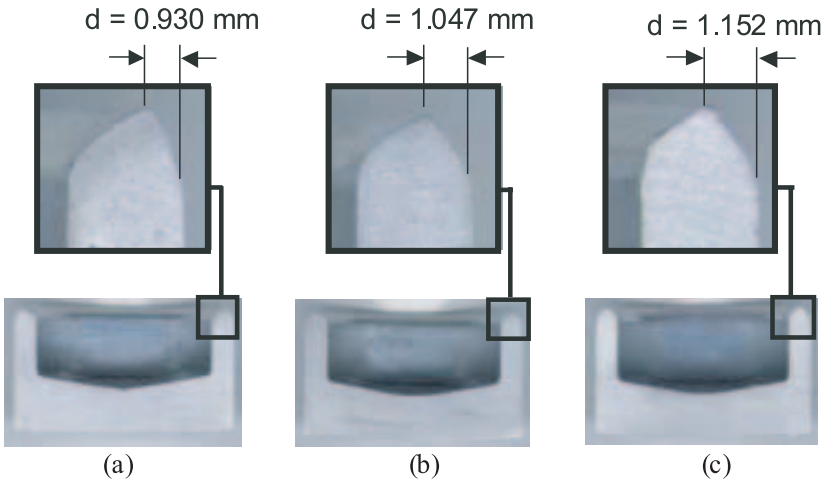

Fig. 3 Measured radial tip distances from tip test experiments with the Al2024-O specimen using lubricants (a) grease, (b) industrial oil grade VG100, and (c) VG 32

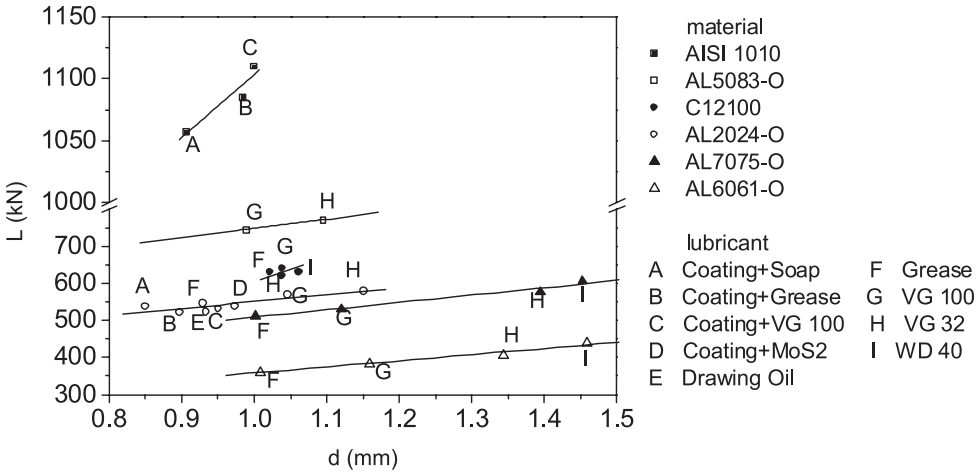

Fig. 4 Plots of L versus d obtained from experiments with various materials and lubricants

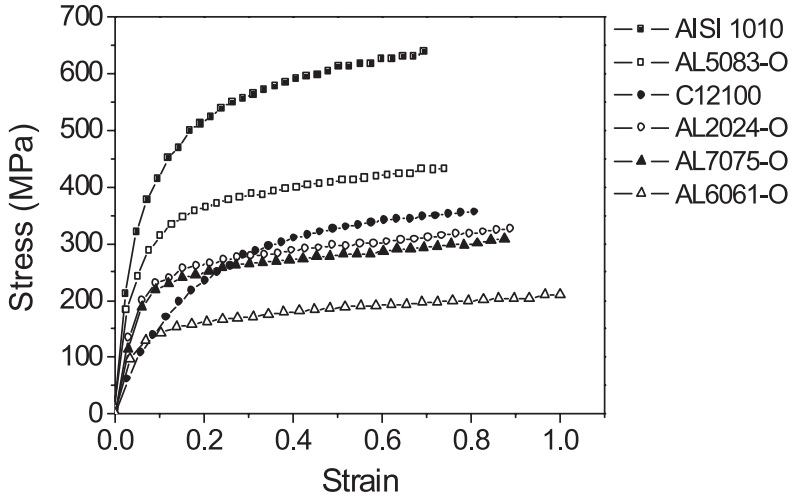

Fig. 5 Stress–strain curves obtained from compression tests on various materials

and measurements of the radial tip distance were made at four locations of each specimen.

Figure 4 shows the plots of L versus d obtained from the experiments using various materials and lubricants. As can be seen in this figure, the linear relationships between L and d were maintained regardless of the tested materials. However, for pure copper it can be seen that the

range of deviation of the measured values of L and d according to various lubricants were relatively small compared with those for other materials.

3 EFFECT OF STRAIN HARDENING

FE simulations using CAMP*form*-2D [**9**–**11**] were carried out for numerical investigations to determine the shear friction factor and material properties using the tip test. The flow stress equations ($\overline{\sigma} = K\overline{\varepsilon}^n$) of the aforementioned materials were obtained through compression tests carried out using the cylindrical specimen with the same dimension for the tip test. The flat dies used in compression tests were made of tool steel alloy AISI D2 and polished to 0.05 μm in R_a and coated with chromium.

Figure 5 shows the resultant stress–strain curves for the investigated materials and Table 1 summarizes the characterized flow stress equations obtained from the compression tests.

Table 1 Comparison of material properties k and n obtained from the compression and tip tests

	Compression test		Tip test	
Material	K (MPa)	n	K (MPa)	n
Al2024-O	330.10	0.140	327.0	0.141
Al5083-O	448.42	0.132	442.0	0.129
Al6061-O	210.62	0.162	212.0	0.167
Al7075-O	309.10	0.140	303.0	0.139
AISI 1010	667.30	0.141	655.0	0.142
C12100	379.50	0.230	379.5	0.230

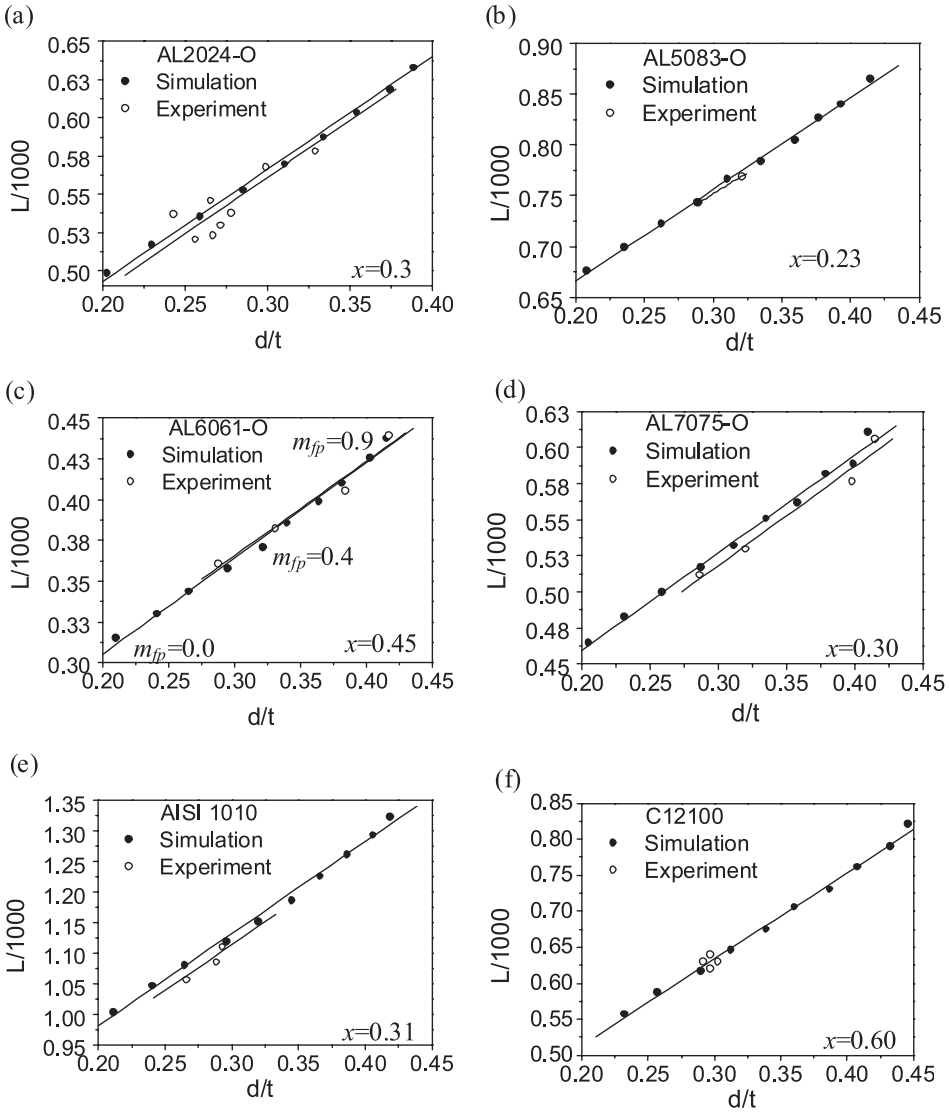

Fig. 6 Comparisons of $L/1000$ versus d/t plots between experiments and simulations with various x values for different materials: (a) Al2024-O; (b) Al5083-O; (c) Al6061-O; (d) Al7075-O; (e) AISI 1010; (f) C12100

It was found from earlier studies [**6**, **7**] that the friction condition at the workpiece–punch interface should be modelled to be higher than that at the workpiece–lower die interface for the backward extrusion process. Thus, the shear friction factor m_{fd} at the workpiece–lower die interface was assumed to be a certain percentage of the shear friction factor m_{fp} at the workpiece–punch interface. That is, the ratio x of the shear friction factors was defined as m_{fd}/m_{fp}, where $0.0 \leq x \leq 1.0$. The detailed procedure of obtaining the value of x can be found in the literature [**6**].

The values of the ratio x of shear friction factors obtained for various materials are shown in Fig. 6. In this figure, the maximum forming load L and tip distance d have been non-dimensionalized by 1000 kN and by the thickness t of the extruded end of the workpiece (3.5 mm) respectively. It can be seen that $x = 0.30$, 0.23, 0.45, 0.30, 0.31, and 0.60 result in the best fit with experimental measurements in terms of the slope for the materials Al2024-O, Al5083-O, Al6061-O, Al7075-O, AISI 1010, and C1200 respectively. These results confirm that the friction at the workpiece–punch interface is higher than that at the workpiece–die interface in the backward extrusion process. Also, it can be seen in this figure that $L/1000$ and d/t have a linear relationship depending on the various shear friction factors determined.

From the current numerical investigation, it was revealed that the ratio x of shear friction factors can be related to the strain-hardening exponent n of the material. For the materials Al2024-O and Al7075-O, whose strain-hardening exponents n were both found to be 0.140, it was found that they also shared a common x value of 0.30. For Al5083-O, Al6061-O, AISI 1010, and C12100, whose respective n values were 0.132, 0.162, 0.141, and 0.230, the corresponding x values were determined to be 0.23, 0.45, 0.31 and 0.60. This relationship between x and n is plotted in Fig. 7. It can be seen from this figure that x increases logarithmically with increasing n in equation (3). Thus, once n is determined from the compression test, x can simply be calculated from the equation

$$x = 1.004 + 0.182 \times \ln(n - 0.118) \tag{3}$$

for the material whose n is larger than 0.118.

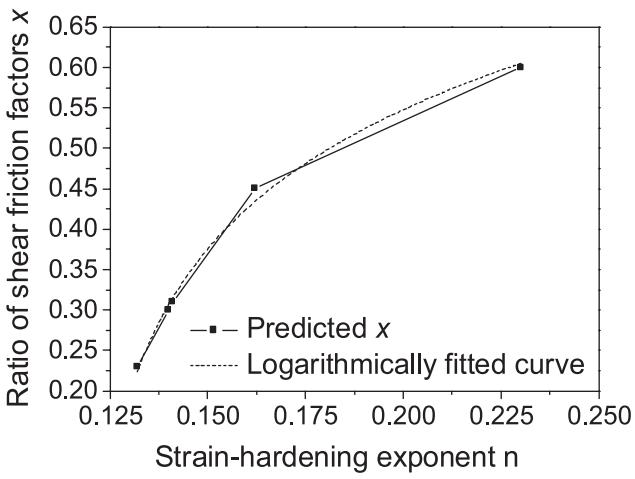

Fig. 7 Logarithmic relation between x and n

4 MATERIAL CHARACTERIZATION BY THE TIP TEST

Although the graphs obtained from experiments and simulations shown in Fig. 6 were parallel in terms of the slope, small gaps exist between the two results. The overall differences in $L/1000$ between the experimental and simulation results were about 1.0, 0.6, 0.43, 1.2, 1.8, and 0.0 per cent respectively, and for d/t the differences about 2.4, 1.5, 0.15, 4.0, 4.8, and 0.0 per cent respectively, for the aforementioned tested materials. It might be construed that this error was caused by the friction effect between the platten and workpiece interfaces during material characterization using the conventional compression test.

However, it is possible to obtain the strength coefficient K, strain-hardening exponent n, and shear friction factor m_f simultaneously using the linear relationship between $L/1000$ and d/t according to the present investigation. This approach decouples the friction effect in the material property

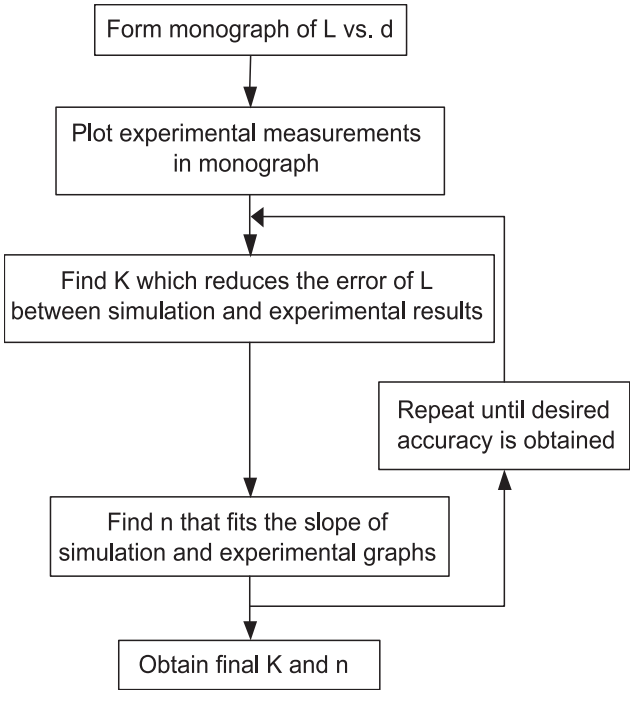

Fig. 8 Procedure for material characterization by the tip test

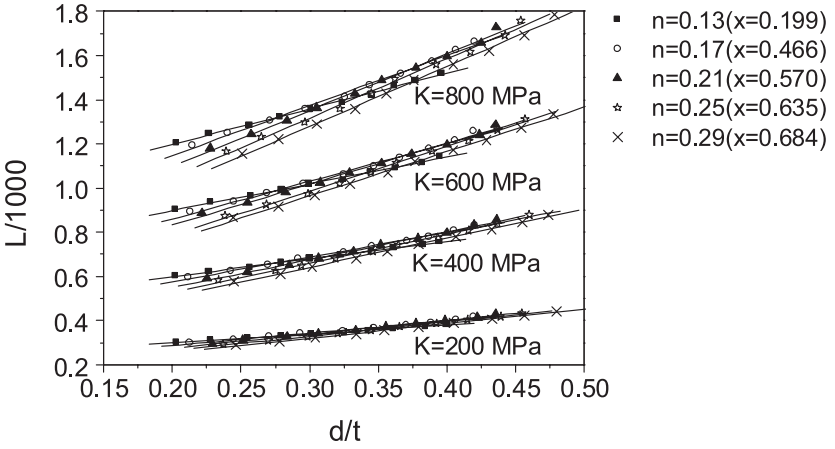

Fig. 9 Monograph of $L/1000$ versus d/t plots for material property measurement

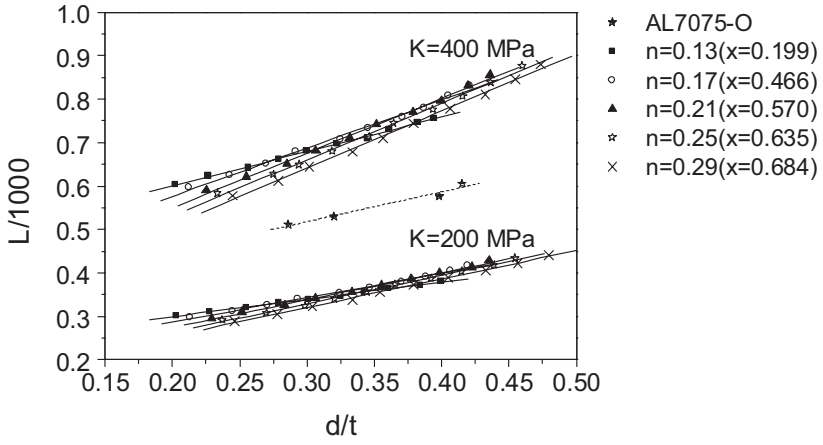

Fig. 10 $L/1000$ versus d/t plots for material characterization of Al7075-O

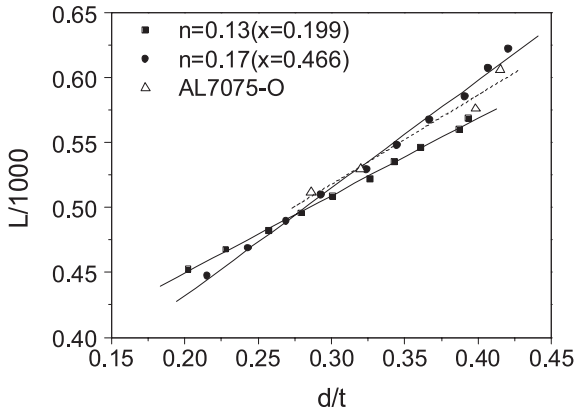

Fig. 11 Comparison of $L/1000$ versus d/t plots obtained from experiment with Al7075-O and simulations with $K = 300$ MPa and $n = 0.13$ and 0.17

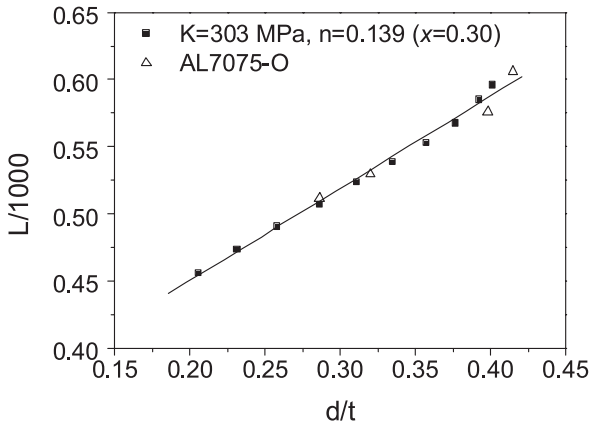

Fig. 12 Comparison of $L/1000$ versus d/t plots obtained from experiment with Al7075-O and simulations with $K = 303$ MPa and $n = 0.139$

measurement compared with the conventional compression test.

Figure 8 shows the overall procedure for determining the material property by using the tip test. First, a single graph of non-dimensionalized maximum forming load versus tip distance curves according to K and n values was prepared. For this, various FE simulations were carried out with K in the range 100–800 MPa in increments of 200 MPa and n in the range 0.13–0.29 in increments of 0.04. The value of x was determined from the logarithmic relation (3). The resultant

graph showing $L/1000$ versus d/t curves is shown in Fig. 9.

For material characterization of Al7075-O, the experimentally obtained values of $L/1000$ and d/t were plotted in the graph shown in Fig. 10. It can be seen that the $L/1000$ versus d/t curve of Al7075-O was located in between the simulation results using K values of 200 and 400 MPa. Thus, simulations with a K value of 300 MPa, which was the average of these values, and an n value of 0.13 were carried out.

The results are compared with the experimental results in Fig. 11. As shown in this figure, although the overall ranges of $L/1000$ values obtained from the simulation and experiment are similar, the error between the slopes needs to be minimized. Since the slope of the $L/1000$ versus d/t graphs was influenced by the strain-hardening exponent n, the simulation using an n value of 0.17 with a fixed K value of 300 MPa was carried out and plotted in Fig. 11. It can be seen that the slope of the $L/1000$ versus d/t graph was increased by this

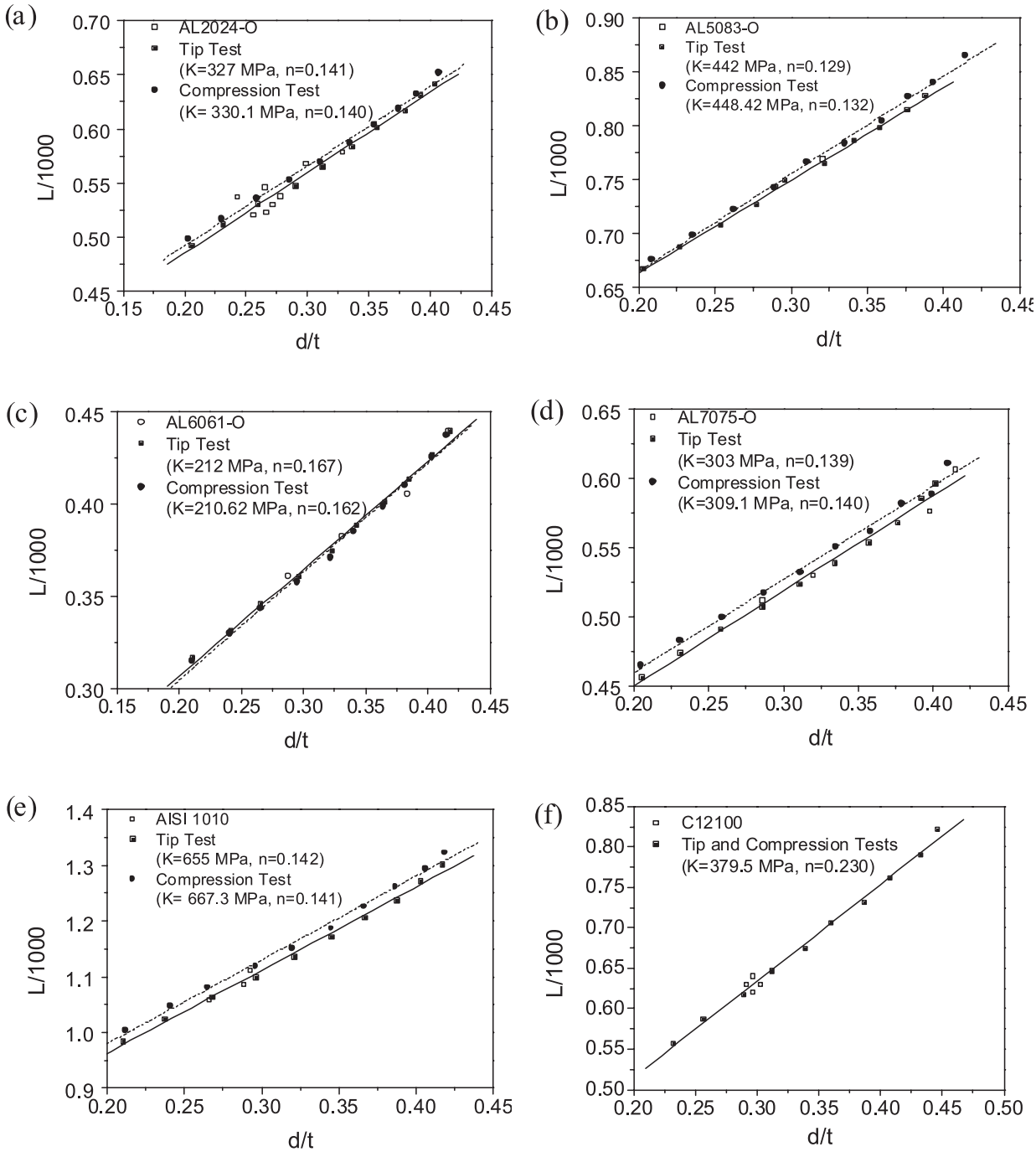

Fig. 13 Comparisons of $L/1000$ versus d/t plots for material properties obtained by tip tests and compression tests: (a) Al2024-O; (b) Al5083-O; (c) Al6061-O; (d) Al7075-O; (e) AISI 1010; (f) C12100

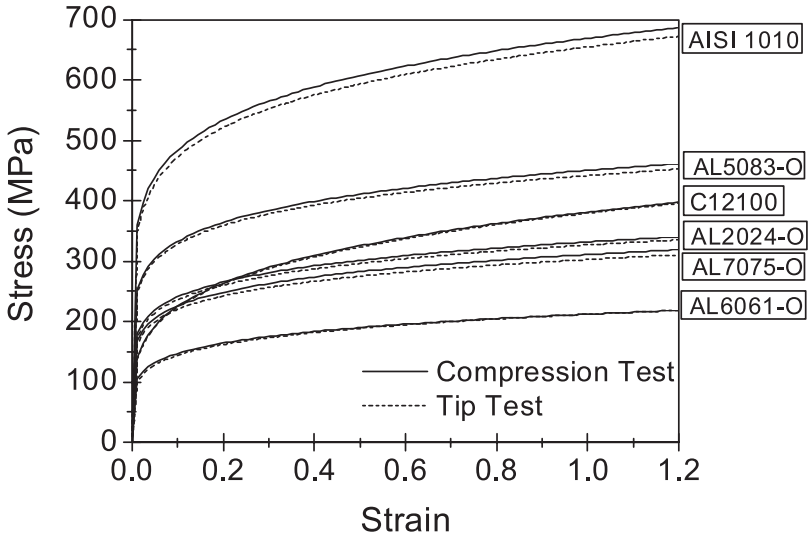

Fig. 14 Comparison of material properties obtained from tip tests and conventional compression tests

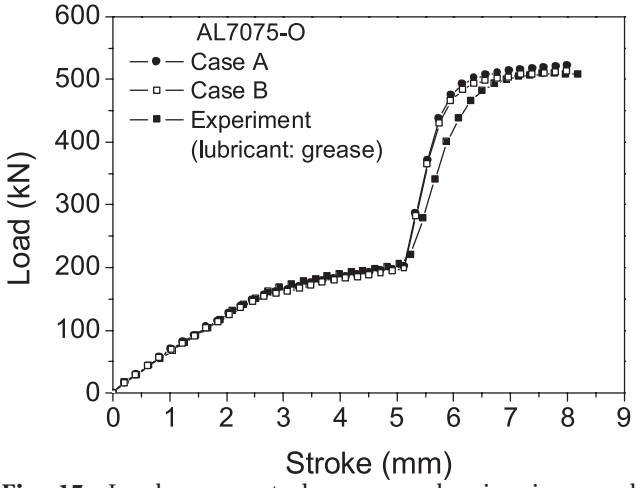

Fig. 15 Load versus stroke curves showing improved accuracy of material properties found by the tip test

adjustment. In a similar manner, by adjusting K and n values in the simulations, it is possible to obtain the $L/1000$ versus d/t graph that matches the experimental results better. For the case of Al7075-O, simulations with $K = 303$ MPa and $n = 0.139$ were found to offer the best fit with experiments, as shown in Fig. 12.

Material characterizations for the other materials were made in the same way and the results are given in Fig. 13. It can be seen that these newly obtained material properties reduce the error of load requirement between experimental and simulation results compared with the simulation results based on the material properties obtained by compression tests. The flow stress curves and equations directly measured by the compression tests and determined by tip tests due to calibration as previously introduced are shown in Fig. 14 and summarized in Table 1 respectively.

Since each dimensionless $L/1000$ and d/t plot in Fig. 13 has a corresponding shear friction factor value, these graphs can be directly converted into shear friction factor versus radial tip distance curves according to the linearity between these two. This conversion leads to the linear equations

$$m_{\text{fp}} = 4.37d/t - 0.94 \quad \text{for Al2024-O} \tag{4}$$

$$m_{\text{fp}} = 4.74d/t - 0.99 \quad \text{for Al5083-O} \tag{5}$$

$$m_{\text{fp}} = 4.28d/t - 0.94 \quad \text{for Al6061-O} \tag{6}$$

$$m_{\text{fp}} = 4.38d/t - 0.93 \quad \text{for Al7075-O} \tag{7}$$

$$m_{\text{fp}} = 4.23d/t - 0.93 \quad \text{for AISI 1010} \tag{8}$$

$$m_{\text{fp}} = 4.11d/t - 0.97 \quad \text{for C12100} \tag{9}$$

The shear friction factors for the lubricants used in the current study as estimated by the above equations are summarized in Tables 2 and 3. Here, the average values of d/t were used in calculating m_{fp} for each lubricant, and the values of m_{fd} were calculated from the relation of x.

For further examination of the material properties and shear friction factors predicted by the tip test, the load versus stroke curve for the tip test with Al7075-O using grease is compared in Fig. 15 with previous results based on the data obtained by the compression test. Case A in this figure indicates the simulation result using $K = 309.1$ MPa and $n = 0.140$ obtained from the compression test, while case B indicates the simulation result using $K = 303$ MPa and $n = 0.139$ obtained from the tip test. m_{fp} for case B was 0.33 given by equation (7) and m_{fp} used in case A was 0.32 obtained from Fig. 6(d). As can be seen in Fig. 15, the load prediction of case B is in

Table 2 Predicted shear friction factors obtained from tip tests with various aluminium alloys

	Al2024-O			Al5083-O			Al6061-O			Al7075-O		
Lubricant	d/t	m_{fp}	m_{fd}	d/t	m_{fp}	m_{fd}	d/t	m_{fp}	m_{fd}	d/t	m_{fp}	m_{fd}
Coating + soap	0.243	0.12	0.04									
Coating + grease	0.256	0.18	0.06									
Coating + VG 100	0.272	0.25	0.08									
Coating + MoS_2	0.278	0.27	0.09									
Drawing oil	0.267	0.23	0.07									
Grease	0.266	0.22	0.07	0.292	0.39	0.07	0.288	0.29	0.13	0.287	0.33	0.10
VG 100	0.299	0.37	0.12	0.321	0.53	0.10	0.331	0.48	0.22	0.320	0.47	0.14
VG 32	0.329	0.50	0.16				0.384	0.70	0.32	0.398	0.81	0.24
WD 40							0.417	0.84	0.38	0.415	0.89	0.27

Table 3 Predicted shear friction factors obtained from tip tests for the materials AISI 1010 and C12100

	AISI 1010			C12100		
Lubricant	d/t	m_{fp}	m_{fd}	d/t	m_{fp}	m_{fd}
Coating + soap	0.266	0.20	0.06			
Coating + grease	0.289	0.29	0.10			
Coating + VG 100	0.293	0.31	0.10			
Grease				0.292	0.23	0.14
VG 100				0.297	0.25	0.15
VG 32				0.297	0.25	0.15
WD 40				0.303	0.28	0.17

better agreement with the experimentally measured load than that of case A. Such an improvement was found for the other tested materials as well.

5 CONCLUSIONS

Tip test experiments were conducted for various materials in the present investigation. It was revealed that the linearity between the non-dimensionalized radial tip distance and maximum forming load was maintained regardless of the material types. It was also found from the present investigation that the friction at the workpiece–die interface was always lower than that at the workpiece–punch interface and that this ratio of shear friction factors increased logarithmically with increase in the strain-hardening level of the material. Finally, material characterization for various materials was successfully made using the tip test. It was shown that the newly obtained material properties led to more accurate simulation results of load requirement than those obtained from conventional compression tests.

ACKNOWLEDGEMENTS

The authors wish to thank the grant of the Components and Materials Technology Development Project from the Ministry of Commerce, Industry, and Energy.

REFERENCES

1 **Kobayashi, S., Oh, S. I.,** and **Altan, T.** *Metal Forming and the Finite Element Method*, 1989 (Oxford University Press, Oxford).
2 **Chen, C.C.** and **Kobayashi, S.** Rigid–plastic finite-element analysis of ring compression. In *Applications of Numerical Methods of Forming Processes* (Eds H. Armen and R. F. Jones), 1978, AMD-Vol. 28, pp. 163–174 (American Society of Mechanical Engineers, New York).
3 **Nakamura, T., Zhang, Z.L.,** and **Kimura, H.** Evaluation of various lubricants for cold forging processes of different aluminum alloys. ICFG Document 2/96, International Cold Forging Group, Emangen, 1996.
4 **Nakamura, T., Bay, N.,** and **Zhang, Z.** FEM simulation of a friction testing method based on combined forward conical can-backward straight can extrusion. *Trans. ASME, J. Tribology*, 1998, **120**(4), 716–723.
5 **Im, Y.T., Cheon, J.S.,** and **Kang, S.H.** Determination of friction condition by geometrical measurement of backward extruded aluminum alloy specimen. *Trans. ASME, J. Mfg Sci. Engng*, 2002, **124**(2), 409–415.
6 **Im, Y.T., Kang, S.H.,** and **Cheon, J.S.** Finite element investigation of friction condition in a backward extrusion of aluminum alloy. *Trans. ASME, J. Mfg Sci. Engng*, 2003, **125**(2), 378–383.
7 **Im, Y.T., Kang, S.H., Cheon, J.S.,** and **Kim, S. Y.** Finite element investigation of tip test with an aluminum alloy. *Japan Soc. Mech. Engng Int. J., S. A*, 2003, **43**(3), 224–229.
8 **Kang, S.H., Lee, J.H., Cheon, J.S.,** and **Im, Y.T.** The effect of strain-hardening on frictional behavior in tip test. *Int. J. Mech. Sci.*, 2004, **46**, 855–869.

9 **Kwak, D.Y., Cheon, J.S.,** and **Im, Y.T.** Remeshing for metal forming simulations: Part 1: two-dimensional quadrilateral remeshing. *Int. J. Numer. Methods Engng*, 2002, **53**(11), 2463–2500.
10 **Hussain, P.B., Cheon, J.S., Kwak, D.Y., Kim, S.Y.,** and **Im, Y.T.** Simulation of clutch hub forging process using CAMP*form*. *J. Mater. Processing Technol.*, 2002, **123**(1), 120–132.
11 CAMP*form*2D Users Manual Version 1.5, 2002; http://camp.kaist.ac.kr/campseries.

APPENDIX

Notation

d distance of the radial tip from the workpiece sidewall
K strength coefficient
L forming load at a punch stroke of 8 mm
m_{fd} shear friction factor at the workpiece–die interface
m_{fp} shear friction factor at the workpiece–punch interface
n strain-hardening exponent
R_a surface roughness
t thickness of the extruded end of the workpiece
x ratio of the shear friction factor of the workpiece–die interface to that of the workpiece–punch interface
$\bar{\varepsilon}$ effective strain
$\bar{\sigma}$ effective stress